Top-quark production by W-gluon fusion

R. K. Ellis and Stephen Parke

Fermi National Accelerator Laboratory, P.O. Box 500, Batavia, Illinois 60510

(Received 13 May 1992)

We present formulas and results on top-quark production by W-gluon fusion. A detailed comparison is made between the rate for this process and the backgrounds at the Fermilab Tevatron. The main backgrounds to this process come from $t\bar{t}$ production and from the production of a W-boson plus jets in QCD. Using standard cuts at the Tevatron and a b-quark tag we find that the $t\bar{b}$ production rate is smaller than at least one of these backgrounds for all top-quark masses accessible at Fermilab.

I. INTRODUCTION

The standard mechanisms to produce a top quark at the Fermilab Tevatron are parton-parton annihilation processes:

$$q + \bar{q} \rightarrow t + \bar{t} , \tag{1}$$

$$g + g \rightarrow t + \bar{t} . \tag{2}$$

For a top quark of mass above $m_t = 100$ GeV at $\sqrt{s} = 1.8$ TeV the quark-antiquark annihilation is the dominant process, because of the stiffness of the quark distribution functions. Top quarks produced by this mechanism will be identified by observing their decay products, either into leptons + jets or into leptons only (e.g., $e\mu$). The identification of the signal requires information about the full final state. This is best calculated using a parton model Monte Carlo program [1].

However, it has been suggested in the literature [2-4] that production by the fusion of a gluon and a W-boson can provide an observable signal for certain energies and mass ranges, because of its characteristic kinematic structure. The W-gluon fusion process, shown in Fig. 1, requires the production of only a single top quark. It is opportune to reexamine this claim both because of the upcoming collider run and because of the theoretical advances since this mechanism was suggested. The theoretical advances include the normal updating of parton distribution functions and the advances in the estimate of the W+jets background [5].
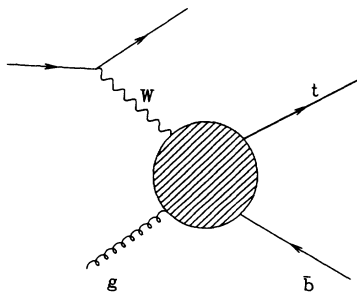
II. MATRIX ELEMENT FOR W-GLUON FUSION

The complete tree-graph calculation, including top-quark decay, is known for $t\bar{t}$ production. Here we provide the corresponding information for the $t\bar{b}$ process. We present the matrix element squared for

$$u + g \rightarrow d + \bar{b} + v + e^+ + b , \tag{3}$$

which proceeds through the production of a top quark. It is convenient to consider the process with all momenta outgoing. the momenta are shown in parentheses:

$$g(-k) \rightarrow \bar{u}(p_1) + d(p_2) + \bar{b}(p_3) + v(q_1)$$
$$+ e^+(q_2) + b(q_3) . \tag{4}$$

The relevant Feynman diagrams are shown in Fig. 2. The top quark is denoted by a heavy line. To simplify the notation we write

$$p = p_1 + p_2 + p_3, \quad q = q_1 + q_2 + q_3 , \tag{5}$$

$$d(p) = p^2 - m_t^2, \quad w(q) = q^2 - m_W^2 . \tag{6}$$

The masses of the top and the bottom quarks are denoted by m_t and m_b. We define the transition probability for the unphysical process, Eq. (4):

$$T(p_1, p_2, p_3, q_1, q_2, q_3, k)$$
$$= \frac{a_{11} + a_{22} + a_{33} + a_{12} + a_{23} + a_{13}}{[w(p_1 + p_2)w(q_1 + q_2)]^2} . \tag{7}$$

In terms of the function T, the invariant matrix element squared for the physical process averaged (summed) over initial (final) colors and spins is

$$\sum |M|^2 = 2^{13} \pi \alpha_s G_F^4 M_W^8 T(-p_1, p_2, p_3, q_1, q_2, q_3, -k) . \tag{8}$$
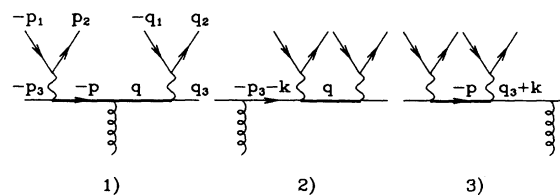
The a_{ij}'s are defined as

FIG. 2. Diagrams for $t\bar{b}$ production.

FIG. 1. The W gluon fusion process.

$$a_{11} = \frac{q_1 \cdot q_3 p_1 \cdot p_3}{[d(p)d(q)]^2}\{2[d(p)+d(q)]p_2 \cdot p q_2 \cdot q - d(p)d(q)p_2 \cdot q_2 + q^2(2p_2 \cdot p p \cdot q_2 - m_t^2 p_2 \cdot q_2) + p^2(2q_2 \cdot q q \cdot p_2 - m_t^2 p_2 \cdot q_2)\} ,$$

(9)

$$a_{22} = \frac{q_1 \cdot q_3}{2[p_3 \cdot k d(q)]^2}\{S(p_2,q,q_2,q)[m_b^2(p_1 \cdot k + p_1 \cdot p_3) - p_1 \cdot k p_3 \cdot k)]\} ,$$

(10)

$$a_{12} = \frac{q_1 \cdot q_3}{2p_3 \cdot k d(p)[d(q)]^2}\{(2p_1 \cdot p_3 + p_1 \cdot k)[2q_2 \cdot q S(q,p_3,p,p_2) - q^2 S(q_2,p_3,p,p_2) - m_t^2 S(p_3,p_2,q,q_2)]$$

$$+ p_1 \cdot p_3[2q_2 \cdot q S(q,k,p,p_2) - q^2 S(q_2,k,p,p_2) - m_t^2 S(k,p_2,q,q_2)]$$

(11)

$$- p_3 \cdot k[2q_2 \cdot q S(q,p_1,p,p_2) - q^2 S(q_2,p_1,p,p_2) - m_t^2 S(p_1,p_2,q,q_2)]$$

$$+ 2q_2 \cdot q G(k,p_2,p;k,p_1,p_3) - q^2 G(p_2,q_2,p;p_1,p_3,k) - m_t^2 G(p_2,q_2,q;p_1,p_3,k)\} ,$$

(12)

$$a_{23} = \frac{1}{2p_3 \cdot k q_3 \cdot k d(p)d(q)}(S(q_2,q,p_2,p)\{q_1 \cdot q_3[p_1 \cdot k p_3 \cdot q_3 + p_1 \cdot p_3(p_3 \cdot q_3 + p_3 \cdot k) - p_1 \cdot q_3 p_3 \cdot k]$$

$$+ p_1 \cdot p_3[q_1 \cdot k p_3 \cdot q_3 + q_1 \cdot q_3(p_3 \cdot q_3 + q_3 \cdot k) - p_3 \cdot q_1 q_3 \cdot k]\}$$

$$+ p_1 \cdot p_3 G(k,p_2,q_2,q;k,q_1,q_3,p_3) + q_1 \cdot q_3 G(k,q_2,p_2,p;k,p_1,p_3,q_3)) ,$$

(13)

where

$$S(p_1,p_2,p_3,p_4) = p_1 \cdot p_2 p_3 \cdot p_4 + p_2 \cdot p_3 p_1 \cdot p_4 - p_1 \cdot p_3 p_2 \cdot p_4$$

(14)

and G is the determinant of the scalar products (the Gram determinant). For example,

$$G(p_1,p_2;q_1,q_2) = p_1 \cdot q_1 p_2 \cdot q_2 - p_1 \cdot q_2 p_2 \cdot q_1 .$$

(15)

The remaining two terms are obtained by symmetry:

$$a_{33} = a_{22}(p \leftrightarrow q) ,$$

$$a_{13} = a_{12}(p \leftrightarrow q) .$$

(16)

The above formula is complete, except that we have ignored the width of the top quark and the W bosons. To correct this, for the decaying top quark and W boson, we multiply the matrix element squared by

$$\frac{d(q)^2 w(q_1+q_2)^2}{[d(q)^2+m_t^2\Gamma_t^2][w(q_1+q_2)^2+m_W^2\Gamma_W^2]} ,$$

(17)

where Γ_t and Γ_W are the widths of the top quark and W boson.

III. NUMERICAL RESULTS

In Fig. 3 we present the total rate for $e^+ + \nu +$ jet production calculated at the tree-graph level. No cuts are performed on the jets. This final state can be reached either by the standard parton-antiparton annihilation process producing $t\bar{t}$ or via the W-gluon fusion process producing a $t\bar{b}$ intermediate state. In both cases the t quark decays to e^+, ν, and b quark. In real life the rates will be larger when we take into account other final states involving e^-, μ^+, and μ^-. In the following we will only consider the final state containing an e^+ in all curves.
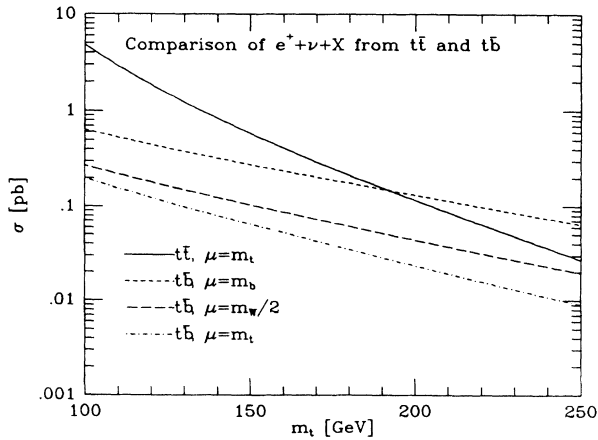

FIG. 3. Comparison of total rate for $e^+ + \nu +$ jets production from $t\bar{t}$ and $t\bar{b}$ production at tree-graph level.
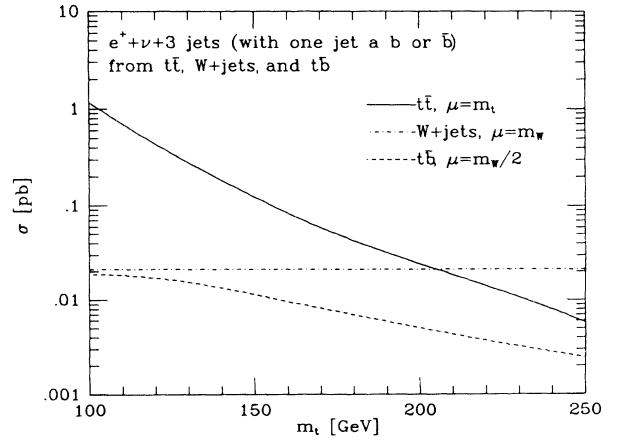

FIG. 4. Comparison of total rate for $e^+ + \nu + 3$ jet production from $t\bar{t}$, $W +$ jets, and $t\bar{b}$ production.
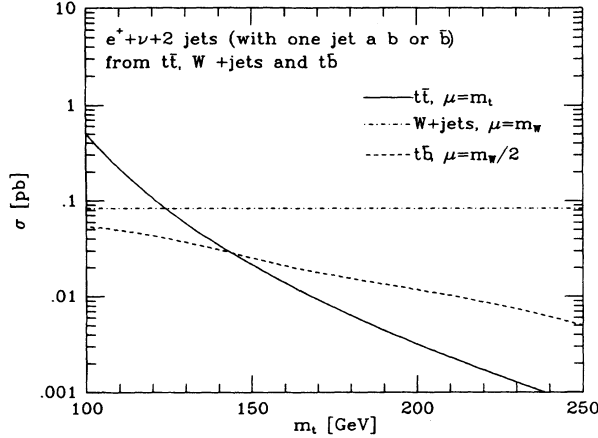
FIG. 5. Comparison of total rate for $e^+ + \nu + 2$ jet production from $t\bar{t}$, $W+$ jets, and $t\bar{b}$ production.

Figure 3 indicates that the W-gluon fusion process may be competitive, especially for larger values of the top-quark mass. Note that there is a considerable theoretical uncertainty in all rates quoted in this paper because of the choice for the QCD scale μ. This is a consequence of performing calculations at the tree-graph level. The range of variation is displayed in Fig. 3 for the W-gluon fusion process. In the case of the parton-parton annihilation to produce $t\bar{t}$ this uncertainty also exists. The curves shown are the result of the tree-graph calculation [1]. Higher-order corrections [6–9] indicate that the choice $\mu = m_t$ which we make in this paper is at the lower end of the range of predictions. The cross section may be as much as 30% higher. Our phenomenological predictions are obtained as follows. The parameters which we use are $m_W = 80$ GeV and $m_b = 5$ GeV. We use the Harriman-Martin-Roberts-Stirling (HMRS) structure functions [10] with $\Lambda_{\overline{MS}} = 0.19$ GeV, where $\overline{MS}$ denotes the modified minimal subtraction scheme. This gives a value of $\alpha_s(M_Z) = 0.108$.

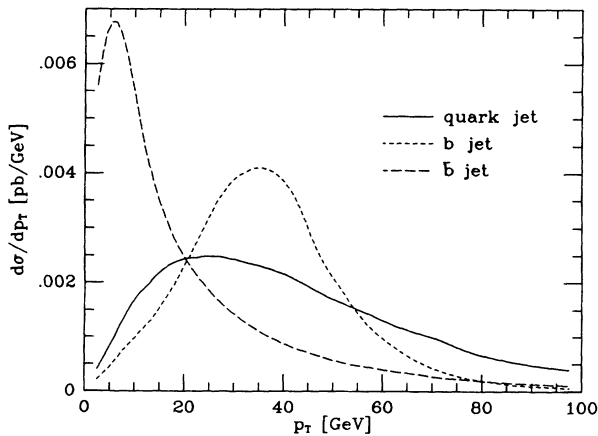The situation is modified once we impose cuts. We use standard Collider Detector at Fermilab Collaboration

FIG. 6. Transverse momentum distributions of final-state quarks in the $t\bar{b}$ process for a top-quark mass of 130 GeV.
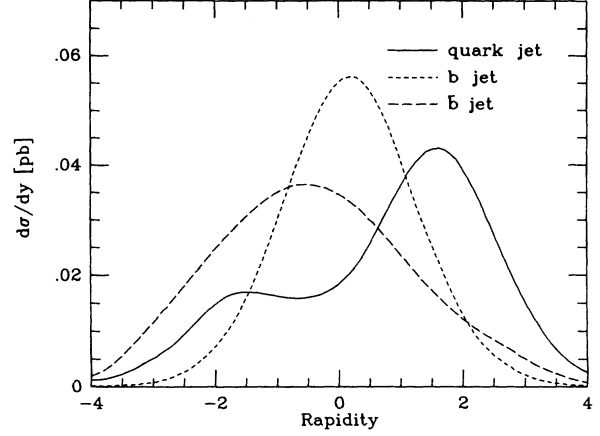

FIG. 7. Rapidity distributions of final-state quarks in the $t\bar{b}$ process for a top-quark mass of 130 GeV.

cuts:

$$|\eta^e| < 1, \quad |\eta^j| < 2, \quad E_T^l > 20 \text{ GeV},$$
$$E_T^j > 15 \text{ GeV}, \quad \Delta R^{jj} > 0.7 .$$
(18)

For definiteness we have chosen $\mu = m_W/2$ when calculating the $t\bar{b}$ cross section in the following figures. Figure 4 shows the rate for $W+$ three jets, with the additional requirement that one of the jets should be a b or $\bar{b}$. The b-quark tagging efficiency is assumed to be 100% with no misidentifications. Once we impose jet cuts we can also compare the QCD production of jets calculated using the program of Ref. [5]. The $t\bar{b}$ production is seen to be much smaller than the $t\bar{t}$ production, for all values of the top-quark mass. It is also smaller than the QCD $W+$ jets production. Figure 5 shows the rate of $W+$ two jets, with the additional requirement that one of the jets should be a b or $\bar{b}$. Here the $t\bar{b}$ production rate is smaller than the QCD $W+$ jets for all values of the top-quark mass.

The standard jet cuts remove a large part of the $t\bar{b}$ sample because the $\bar{b}$ jet is mainly produced at low p_T (see Fig. 6) and the quark jet is produced at large rapidity (see Fig. 7). In Ref. [4] it is argued that these features of the $t\bar{b}$ production mechanism can be used to identify $t\bar{b}$ events. However, at the Tevatron the overall rates are small.

In conclusion, although the total rate for $t\bar{b}$ production is comparable to $t\bar{t}$ production for top-quark masses near 200 GeV at the Tevatron, once standard cuts are imposed on the $e^+ + \nu + 3$ jet events, including a b or $\bar{b}$ tag, the signal is dominated by events from $t\bar{t}$. In the $e^+ + \nu + 2$ jet channel the QCD $W+2$ jet process dominates even with the requirement of a b or $\bar{b}$ in the final state. Also, the rates for the signal $e^+ + \nu +$ jets from the $t\bar{b}$ process are very small at the Tevatron (≈ 10 fb for a top quark mass of 200 GeV) making further selection cuts impossible.

[1] R. Kleiss and W. J. Stirling, Z. Phys. C **40**, 419 (1988).

[2] S. Dawson, Nucl. Phys. **B249**, 42 (1985); S. Dawson and S. Willenbrock, *ibid*. **B284**, 449 (1987).

[3] S. Willenbrock and D. Dicus, Phys. Rev. D **34**, 155 (1986).

[4] C. P. Yuan, Phys. Rev. D **41**, 42 (1990).

[5] F. A. Berends *et al.*, Nucl. Phys. **B357**, 32 (1991).

[6] P. Nason, S. Dawson, and R. K. Ellis, Nucl. Phys. **B303**, 607 (1988).

[7] G. Altarelli *et al.*, Nucl. Phys. **B308**, 724 (1988).

[8] W. Beenaker, H. Kuijf, W. L. van Neerven, and J. Smith, Phys. Rev. D **40**, 54 (1989); W. Beenakker, W. L. Neerven, R. Meng, G. Schuler, and J. Smith, Nucl. Phys. **B351**, 507 (1991).

[9] R. K. Ellis, Phys. Lett. B **259**, 495 (1991).

[10] P. N. Harriman, A. D. Martin, R. G. Roberts, and W. J. Stirling, Phys. Rev. D **42**, 798 (1990). The HMRS set B that we use was revised in April 1990; A. D. Martin, R. G. Roberts, and W. J. Stirling, Phys. Rev. D **37**, 1161 (1988).